materials

MDPI

Article

Effect of TiO_2 Coating on Structure and Electrochemical Performance of $LiNi_{0.6}Co_{0.2}Mn_{0.2}O_2$ Cathode Material for Lithium-Ion Batteries

Lin Li [1,*,†], Zhongyu Li [2,†], Zhifan Kuang [2], Hao Zheng [2], Minjian Yang [1], Jianwen Liu [2], Shiquan Wang [2,3,*] and Hongying Liu [2,3]

[1] School of Chemical Engineering, Guizhou University of Engineering Science, Bijie 551700, China; honglinymj@163.com
[2] Collaborative Innovation Center for Advanced Organic Chemical Materials Co-Constructed by the Province and Ministry, Ministry of Educational Key Laboratory for the Synthesis and Application of Organic Functional Molecules, College of Chemistry and Chemical Engineering, Hubei University, Wuhan 430062, China; 202321106011493@stu.hubu.edu.cn (Z.L.); kzf18720677606@163.com (Z.K.); zhengaho1986@126.com (H.Z.); jianwen@hubu.edu.cn (J.L.); liuhy@hubu.edu.cn (H.L.)
[3] Hubei Three Gorges Laboratory, Yichang 443008, China
* Correspondence: lilin_bj2024@163.com (L.L.); wsqhao@hubu.edu.cn (S.W.)
† These authors contributed equally to this work.

Abstract: High-nickel ternary $LiNi_{0.6}Co_{0.2}Mn_{0.2}O_2$ (NCM622) is a promising cathode material for lithium-ion batteries due to its high discharge-specific capacity and energy density. However, problems of NCM622 materials, such as unstable surface structure, lithium–nickel co-segregation, and intergranular cracking, led to a decrease in the cycling performance of the material and an inability to fully utilize high specific capacity. Surface coating was the primary approach to address these problems. The effect of TiO_2 coating prepared by the sol–gel method on the performance of $LiNi_{0.6}Co_{0.2}Mn_{0.2}O_2$ was studied, mainly including the morphology, cell structure, and electrochemical properties. $LiNi_{0.6}Co_{0.2}Mn_{0.2}O_2$ was coated by TiO_2 with a thickness of about 5 nm. Compared with the pristine NCM622 electrode, the electrochemical performance of the TiO_2-coated NCM622 electrodes is improved. Among all TiO_2-coated NCM622, the NCM622 cathode with TiO_2 coating content of 0.5% demonstrates the highest capacity retention of 89.3% and a discharge capacity of 163.9 mAh g^{-1}, in contrast to 80.9% and145 mAh g^{-1} for the pristine NCM622 electrode, after 100 cycles at 0.3 C between 3 and 4.3 V. The cycle life of the 5 wt% TiO_2-coated NCM622 electrode is significantly improved at a high cutoff voltage of 4.6 V. The significantly enhanced cycling performance of TiO_2-coated NCM622 materials could be attributed to the TiO_2 coating layer that could block the contact between the material surface and the electrolyte, reducing the interface side reaction and inhibiting the transition metal dissolution. At the same time, the coating layer maintained the stability of layered structures, thus reducing the polarization phenomenon of the electrode and alleviating the irreversible capacity loss in the cycle process.

Keywords: $LiNi_{0.6}Co_{0.2}Mn_{0.2}O_2$; TiO_2; surface coating; cyclic performance; lithium-ion batteries

Citation: Li, L.; Li, Z.; Kuang, Z.; Zheng, H.; Yang, M.; Liu, J.; Wang, S.; Liu, H. Effect of TiO_2 Coating on Structure and Electrochemical Performance of $LiNi_{0.6}Co_{0.2}Mn_{0.2}O_2$ Cathode Material for Lithium-Ion Batteries. *Materials* **2024**, *17*, 6222. https://doi.org/10.3390/ma17246222

Academic Editor: Jesus Canales-Vazquez

Received: 30 October 2024
Revised: 9 December 2024
Accepted: 9 December 2024
Published: 19 December 2024

1. Introduction

With the increasing consumption of fossil fuels, the development of a green industrial revolution and the use of clean, renewable energy to achieve carbon substitution have become an inevitable trend, while the development and promotion of renewable energy are also inseparable from reliable energy storage devices [1]. As a kind of high efficiency and cheap energy storage equipment, lithium-ion batteries (LIBs) are widely used in various industries, especially electric vehicles and portable electronics, with the advantages of high energy density, small size, light weight, no memory effect, low self-discharge, and long life compared with traditional secondary batteries [2,3]. The cathode materials play a

crucial role in the electrochemical performance of LIBs, so good stability, high operating voltage, safety, low cost, and high capacity cathode material have to be developed, matching high-performance LIBs [4,5].

High nickel ternary $LiNi_{0.6}Co_{0.2}Mn_{0.2}O_2$ (NCM622) is a promising cathode material for lithium-ion batteries due to its high discharge specific capacity and energy density [6]. However, there are still some key challenges in the production, cycling, and multiplication performance of this material (such as low coulombic efficiency, low thermal stability, low structural stability, microcracks, interfacial side reactions, etc.), which limits their further application [7]. This is mainly attributed to (1) Li^+/Ni^{2+} cation mixing problems due to similar ionic radii. This can trigger a phase transition and reduce the capacity of $LiNi_{0.6}Co_{0.2}Mn_{0.2}O_2$ [8]. (2) Li^+ on the surface of $LiNi_{0.6}Co_{0.2}Mn_{0.2}O_2$ reacts with air to form alkaline impurities such as Li_2CO_3 and LiOH, which accelerates the decomposition of the electrolyte and the formation of HF, causing damage to the electrode [9]. In addition, due to the presence of high-valent Ni ion, the surface structure of the cathode material is unstable and is prone to side reactions with the electrolyte, while the grain boundaries of the cathode particles are prone to cracking, which makes the capacity of lithium-ion batteries decay more quickly [10,11].

A large number of studies have shown that suitable surface modification can play a role in stabilizing the surface chemistry and structure of the material and is also an effective method to enhance the electrochemical performance of ternary materials [12]. Coating materials have proven to be significantly effective, including non-metallic C [13], metal oxides (TiO_2, Al_2O_3) [14], $MgHPO_4$ [15], ZrO_2 [16,17], Li_2SnO_3 [18], fluorides AlF_3 [19], LaF_3 [20], $AlPO_4$ [21], Li_3PO_4 [22], $Mn_3(PO_4)_2$ [23], etc. A portion of the work on NCM-622 material coating modification is shown in Table S1. Yang et al. [24] found that the side reaction between cathode material and electrolyte was effectively suppressed due to the appropriate amount of Sm_2O_3 coating, and the 0.5 wt% Sm_2O_3 NCM material showed higher cycling stability (88.97% at 1 C after 200 cycles). Under the influence of the synergistic effect of ion doping and $LiNbO_3$ coating, the $LiNbO_3$ coated Mg-doped NCM-622 cathode material exhibits excellent electrochemical performance. Thanks to the $LiNbO_3$ coating, which reduces the effect of surface side reactions, and the Mg^{2+} doping, which stabilizes the structure of the material, the cathode material exhibits excellent long-cycle performance and large-multiplication performance under high-voltage operating conditions [25].

TiO_2 is a competitive cathode coating material due to its unique properties, including abundance, structural stability, and electrochemical inertness [26]. Li et al. [27] showed that an appropriate amount of TiO_2 coating can effectively inhibit the interfacial reaction between the electrode material and electrolyte to improve the structural stability of the material. Wang et al. [28] reported that the TiO_2 coating modification treatment could effectively alleviate the internal cracks, phase transition, and main structure change in single crystal $LiNi_{0.6}Co_{0.2}Mn_{0.2}O_2$ (SC-NCM) material, and the capacity retention rate of SC-NCM electrode material was 87.4% after 200 cycles. Qin et al. [29] reported the preparation of amorphous TiO_2-coated $LiNi_{0.6}Co_{0.2}Mn_{0.2}O_2$ cathode materials using the atomic layer deposition (ALD) technique. The amorphous TiO_2 coating can inhibit the dissolution of metal ions in the $LiNi_{0.6}Co_{0.2}Mn_{0.2}O_2$ material and favor the lithium diffusion of the oxide (187.7 mA hg^{-1} at 0.1 C for the initial discharge capacity). Compared with the pure substance, the modified $LiNi_{0.65}Co_{0.15}Mn_{0.2}O_2$ material showed excellent cycling performance and high-temperature performance through nano-TiO_2 modified treatment. This is mainly due to the fact that the Nano-TiO_2 cladding treatment mitigates the side reactions at the electrode/electrolyte interface, suppresses the irreversible H2/H3 phase transition, and slows down the structural pulverization of the material [30]. Mo et al. [31] obtained TiO_2-modified $LiNi_{0.6}Co_{0.2}Mn_{0.2}O_2$ materials by wet capping. It was found that the Ti ions in the TiO_2 capping layer formed a diffusion layer with different Ti^{4+} concentrations. This diffusion layer with different Ti^{4+} concentrations accelerated the electron and Li^+ migration rates and enhanced the interfacial stability and mechanical strength of the material.

In this study, a uniform TiO_2 coating layer was slowly generated on the surface of coated $LiNi_{0.6}Co_{0.2}Mn_{0.2}O_2$ by slowly hydrolyzing in air, tetrabutyl titanate as a raw material for titanium. The effects of the concentration of tetrabutyl titanate on the morphology, structure, and electrochemical properties of the products were investigated. It was found that tetrabutyl titanate could form a thin TiO_2 layer on the surface of high nickel material. Compared with the unmodified sample, the cycling stability of the TiO_2-modified $LiNi_{0.6}Co_{0.2}Mn_{0.2}O_2$ sample was significantly improved. The specific capacity of 5 wt% TiO_2-coated NCM electrode only decreased from 183.5 mAh g^{-1} to 163.9 mAh g^{-1}, and the capacity retention rate was increased to 89.3%. The TiO_2 coating effectively reduces the occurrence of side reactions at the electrode/electrolyte interface, lowers the interfacial impedance, and reduces the polarization of TiO_2-coated NCM during the cycling process.

2. Materials and Methods

All samples used are analytically pure. $LiNi_{0.6}Co_{0.2}Mn_{0.2}O_2$ cathode materials were synthesized using high-temperature solid phase sintering. The $Ni_{0.6}Co_{0.2}Mn_{0.2}(OH)_2$ precursors (Hunan Zhongwei Technology Co., Ltd., Xiangtan, China) and $LiOH{\cdot}H_2O$ were weighed according to the molar ratio of 1.03:1 and ground in an agate mortar for 0.5 h. The mixture was sintered at 480 °C for 6 h and then at 750 °C for 12 h with a temperature increase rate of 5 °C/min under an O_2 atmosphere. The sintered product is the NCM622 cathode material.

Figure 1 shows the preparation of TiO_2-coated NCM622. An amount of 2 g of NCM622 and tetrabutyl titanate (TBOT, 0.2557 g, 0.6393 g and 1.0655 g corresponds to 2.0, 5.0, and 8.0 wt% TiO_2) were homogeneously dispersed in anhydrous ethanol, then 0.4 mL of $NH_3{\cdot}H_2O$ was added dropwise and stirred for 2.5 h. Then, the obtained powder was collected by centrifugation and washed with deionized water and ethyl alcohol three times, and the above mixture was dried under vacuum at 60 °C for 12 h. Finally, the mixture was annealed at 500 °C for 4 h to produce coating samples. The samples were recorded as 2 wt%, 5 wt%, and 8 wt% TiO_2-NCM, respectively, according to the addition content of TiO_2.

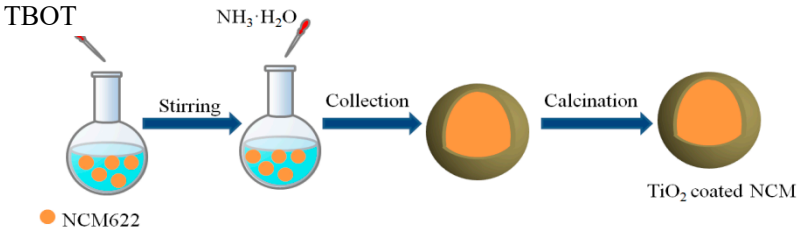

Figure 1. Schematic illustration of synthesis procedure for TiO_2-NCM622.

3. Results and Discussion

Figure 2 shows the X-ray diffraction (XRD) patterns of NCM622 and three modified samples with different amounts of TiO_2 coating. As shown in Figure 2, the diffraction peaks of all samples match well with the standard PDF card (JCPDS, No. 87-1560), which corresponds to the R3m space group of the hexagonal α-$NaFeO_2$ structure [32]. The more obvious splitting of the (006)/(012) and (018)/(110) peaks observed at 38° and 65°, respectively, suggested that the material has a good lamellar structure and also implies that the original structure of the material is well preserved by the capping method used [19]. In addition, no diffraction peaks of TiO_2 were observed in the XRD spectra of the modified samples, which may be due to the small amount of cladding used [20]. It is also observed that compared with the NCM622 bulk sample, the (003) peak and the (104) peak of the modified sample have a leftward shift, and there is no obvious change in the peak intensity of the diffraction peaks, which suggests that for the TiO_2-coated sample, a small amount of Ti^{4+} may have diffused into the structure of the NCM622 bulk phase, broadening the (003) crystal plane spacing [Figure S1a,b] [33].

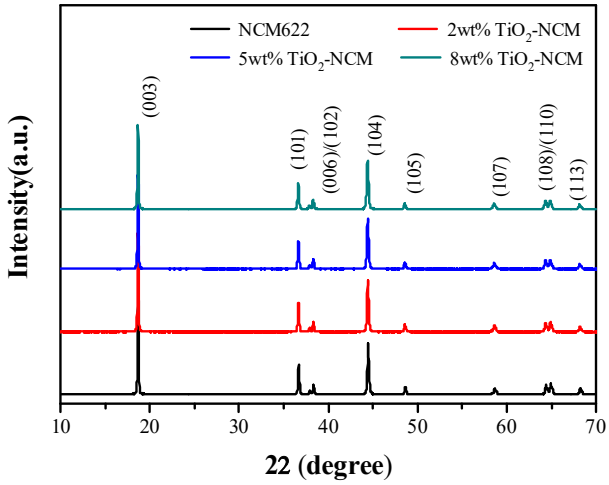

Figure 2. XRD patterns of NCM622 and TiO_2 coated NCM samples.

The cell structure parameters of the pure NCM622 and TiO_2-coated NCM samples were obtained by using a JADE (MDI JADE 6.5) software analyzer. The results can reflect the degree of cation mixing and exclusion in nickel-rich materials. The cell parameters of the pure NCM622 and TiO_2-coated NCM samples are shown in Table 1. The I_{003}/I_{104} value and c/a value are used to assess the degree of Ni/Li mixing in nickel-rich materials. The $I_{(003)}/I_{(104)}$ values of bare MCM622, 2 wt%, 5 wt%, 8 wt% TiO_2-NCM are 1.65, 1.81, 1.83, 1.88, respectively, as shown in Table 1. Compared with the NCM622 bulk sample, the c-axis length of the TiO_2-coated NCM sample is significantly larger, and the Li/Ni mixing degree is increased, which further confirms that part of Ti^{4+} doping enters into the bulk structure of NCM622, and part of Ni^{2+} in the transition metal sites enters into Li^+ due to the charge equilibrium, which increases the Li/Ni mixing degree of the material [14]. In addition, when the c/a value is greater than 4.9, the material is considered to have a complete laminar structure. As can be seen from Table 1, the c/a values of all the samples are greater than 4.9, so it can be determined that four kinds of materials have a complete laminar structure [25]. It is generally believed that a high Li/Ni miscibility will hinder the interlayer Li^+ transport during the charge/discharge process; however, a moderate Li/Ni miscibility can help improve the electrochemical performance of the material [22].

Table 1. The lattice parameters (a and c) and $I_{(003)}/I_{(104)}$ of the NCM622 and TiO_2-coated NCM622 samples.

Sample	Lattice Parameters			$I_{(003)}/I_{(104)}$
	a (Å)	c (Å)	c/a	
NCM622	2.8619	14.1927	4.9592	1.65
2 wt% TiO_2-NCM	2.8642	14.2036	4.9590	1.81
5 wt% TiO_2-NCM	2.8726	14.2497	4.9606	1.83
8 wt% TiO_2-NCM	2.8769	14.2623	4.9575	1.88

The (003) peak of TiO_2-coated NCM samples shifts toward a lower two-theta angle compared with pristine NCM622 bulk, as shown in Figure S1. These subtle structural variations after TiO_2 coating are mainly due to the larger size of the Ti^{4+} in an octahedral environment (r_{Ti4+} = 0.60 Å) as compared to that of Ni^{3+} (r_{Ni3+} = 0.56 Å), Co^{3+} (r_{Co3+} = 0.54 Å), and Mn^{4+} (r_{Mn4+} = 0.53 Å), which suggests the partial Ti^{4+} incorporated into the NCM622 lattice [31,32].

Figure 3 shows the XPS full spectrum of the 5 wt% TiO_2-coated NCM sample, from which it can be observed that there are characteristic peaks of Ni, Co, Mn, C, and O elements on the surface of the material, and there are also characteristic peaks of Ti element on the surface of the 5 wt% TiO_2-coated NCM sample. Figure 3c shows the C 1s spectra,

from which it can be seen that three peaks located at binding energies of 284.8, 286.4, and 289.3 eV were fitted to three peaks, which are attributed to sp2 bonded C-C, C-O, and C=O, respectively. The Ni $2p_{1/2}$ and Ni $2p_{3/2}$ peaks in the 5 wt% TiO_2-coated NCM are located at 872.68 eV and 855.08 eV, respectively; the Mn $2p_{3/2}$ and Mn $2p_{1/2}$ peaks are located at 642.58 eV and 653.98 eV, respectively; and the characteristic peaks at the positions of 780.28 and 795.18 eV correspond to Co $2p_{3/2}$ and Co $2p_{1/2}$, respectively [30]. It can be seen that the TiO_2-coated NCM622 modified material did not change the valence states of Ni, Mn, and Co elements. The characteristic peaks at positions 529.3 eV, 531.6 eV, and 532.5 eV corresponded to O1s. The characteristic peaks of Ti $2p_{3/2}$, Ti $2p_{1/2}$, and TiO_2 appeared in the 5 wt% TiO_2-coated NCM sample at positions located at 458.2 eV, 463.9 eV, and 472 eV (Figure 3g), which indicated the presence of Ti^{4+} on the surface of the 5 wt% TiO_2, which was in agreement with the previous study [31]. Figure S2 is the XPS spectra of bare NCM622. Figure S2a is the survey spectrum of bare NCM622;there are characteristic peaks of Ni, Co, Mn, C, and O elements on the surface of the material. Figure S2b–d are characteristic peaks of Ni 2p, Co 2p, and Mn 2p, respectively, showing similar binding energies with the 5 wt% TiO_2-coated NCM, except without the Ti element.

Figure 4a–d shows the SEM images of NCM622 and TiO_2-coated materials with different TiO_2 amounts. From Figure 4, it can be seen that the particles take on the spherical morphology with a size of 5–10 μm. These microspheres are assembled by particles, as shown in Figure 4a–d. Figure 4e,f is the typical TEM images of a microsphere for 5 wt% TiO_2-NCM. It indicates that TiO_2 coating has no significant effect on the particle size and shape of NCM622. As shown in Figure 4e,f, the surface of the 5 wt% TiO_2-NCM sample is relatively smooth and clean, the particle boundaries are obvious, and the surface of the 5 wt% TiO_2-NCM sample has a relatively uniform titanium dioxide coating layer with a thickness of about 5 nm. The inert TiO_2 coating layer can effectively reduce the contact between the material and the electrolyte, which can reduce the side reactions on the surface of the material and give the cathode material an excellent surface structure and stability [26]. The elemental mapping of 5 wt% TiO_2-NCM microsphere indicates that the distribution of Ni, Co, Mn, O, and Ti elements are on the surface of the sample, as shown in Figure 4g. Additionally, the elemental mapping (Figure 4g) shows that the Ti and O are distributed homogeneously throughout the surface and enter the particle, while most of the Ni, Co, and Mn elements are distributed on the bulk and a few on the layer part of the particle [31]. Figure 4h,i shows the HRTEM images of 5 wt% TiO_2-NCM, demonstrating the TiO_2 coating layer with obvious lattice spacing and NCM interface lattice of 0.45 nm within the TiO_2-NCM sample.The lattice spacing is about 0.351 nm, corresponding to the (101) plane of anatase phase TiO_2. According to the HRTEM images of TiO_2-coated material, the TiO_2 coating layer, the pristine material, and the coating process indicate that there is a joint connection between the TiO_2 coating layer and the pristine material.

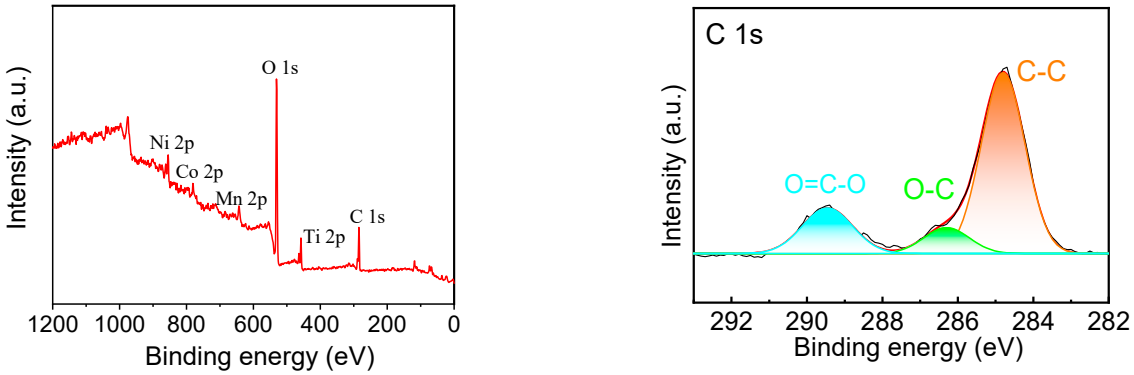

Figure 3. *Cont.*

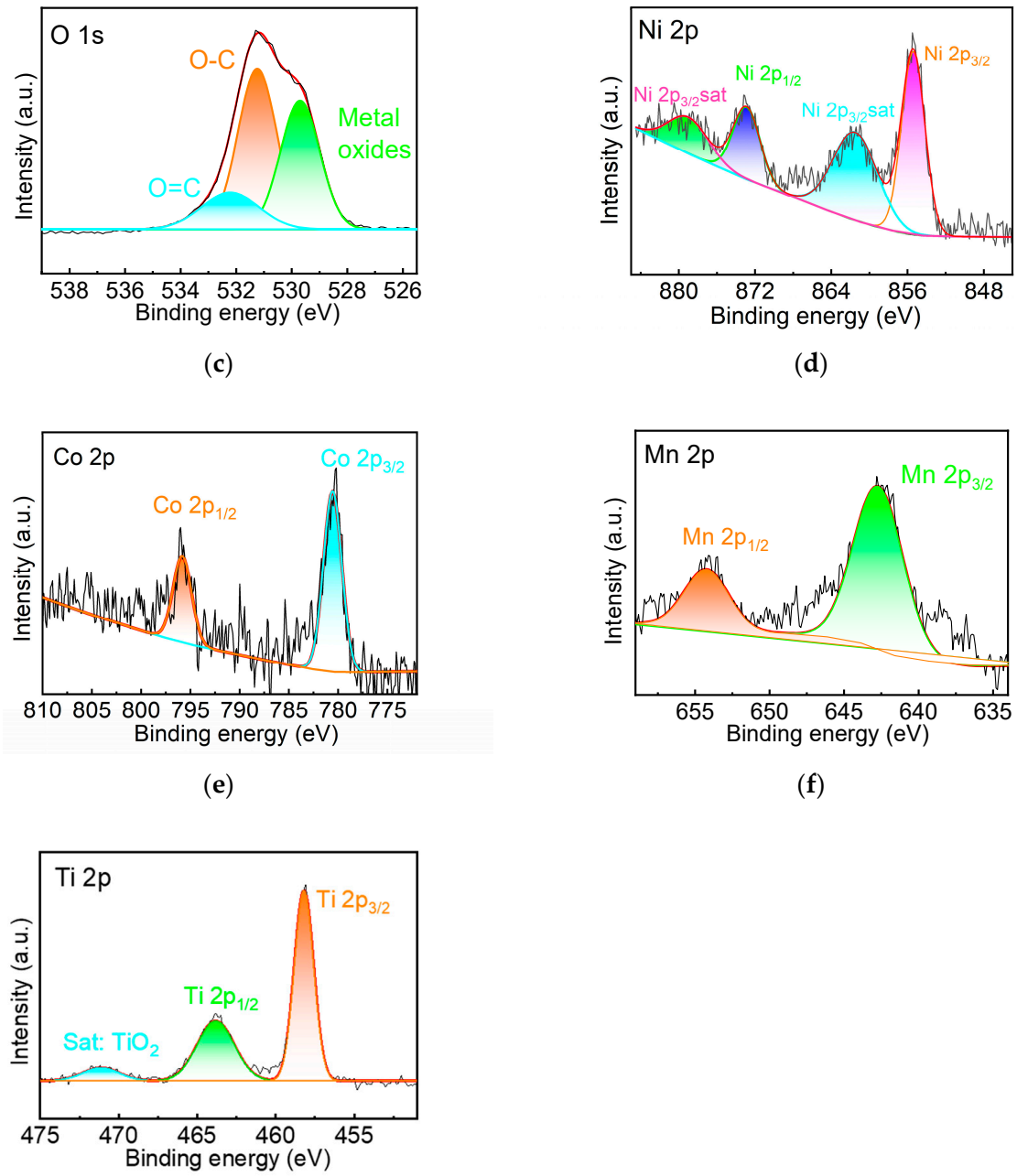

Figure 3. The XPS spectra of 5 wt% TiO_2-NCM: (**a**) survey spectrum, (**b**) C 1s, (**c**) O 1s, (**d**) Ni 2p, (**e**) Co 2p, (**f**) Mn 2p, (**g**) Ti 2p.

Figures S3 and 5 show the cyclic voltammetry (CV) curves of the NCM622 and 5 wt% TiO_2-NCM samples. In the first cyclic voltammetry curve of the NCM622 and 5 wt% TiO_2-NCM, the oxidation process of Ni^{2+}/Ni^{4+} and the anodic delithiation reaction occurred at the oxidation peak position of 3.9~4.1 V, while the reduction process of Ni^{2+}/Ni^{4+} and the anodic lithium embedding reaction occurred at the reduction peak position of 3.55~3.7 V. Compared with the NCM622 sample, the reproducibility of the CV curves of the 5 wt% TiO_2-NCM material is better as the number of scanning turns increases, indicating that the 5 wt% TiO_2-NCM material has excellent cycling stability. In addition, the oxidation peak moves from the high-voltage position in the first turn to the low-voltage direction in the second and third turns, indicating that the first charging and discharging process is an electrochemical activation process for the material to carry out in order to make the

cation arrangement more orderly. This is advantageous for the detachment and embedding of Li ions in the subsequent electrochemical reaction process, which is manifested by the subsequent decrease in the oxidation peak voltage in the second and third turns [30–32].

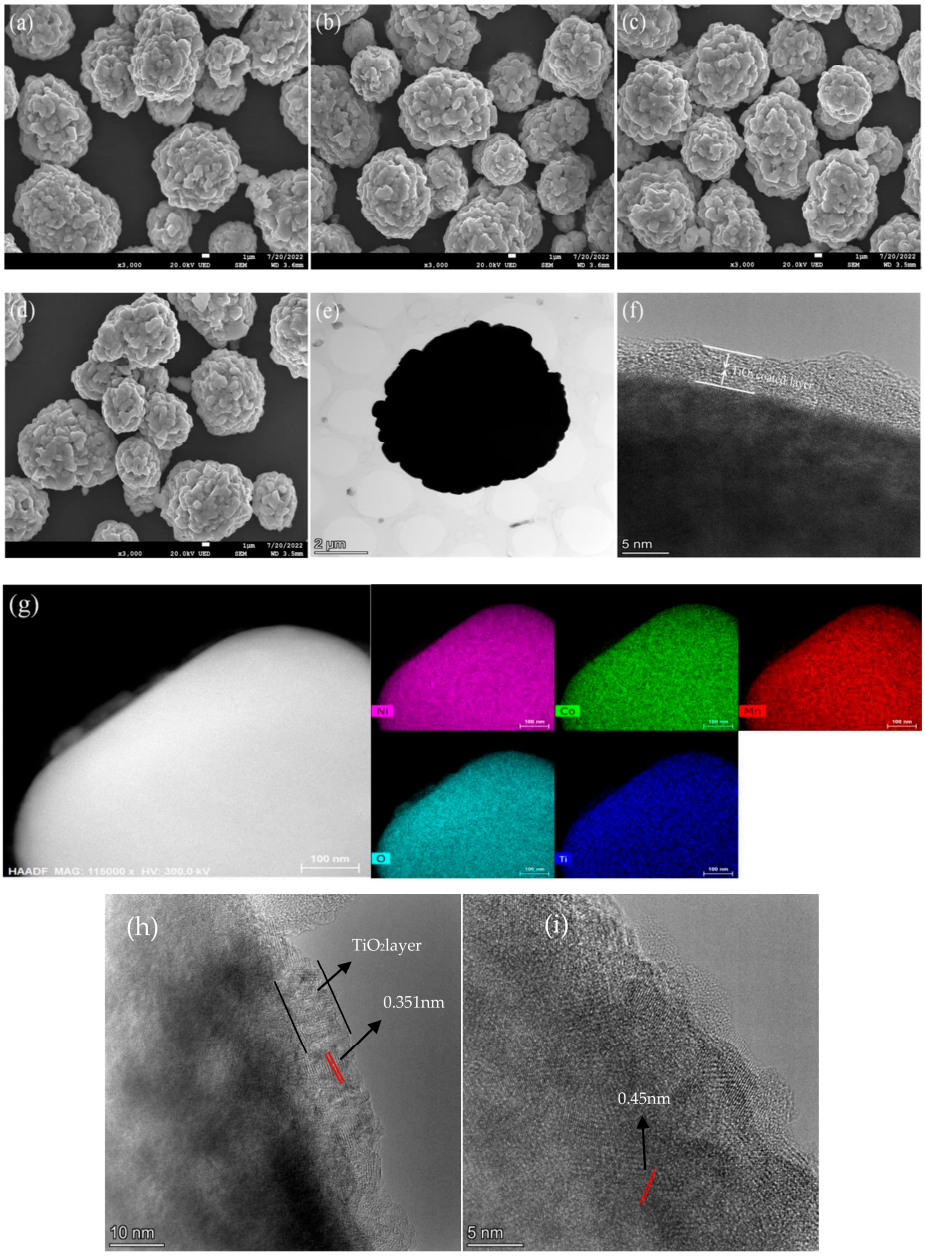

Figure 4. The SEM images of (**a**) NCM622, (**b**) 2 wt% TiO_2-NCM, (**c**) 5 wt% TiO_2-NCM, and (**d**) 8 wt% TiO_2-NCM. (**e**) TEM image of 5 wt% TiO_2-NCM; (**f**) HRTEM image; (**g**) FE-SEM elemental mapping of 5 wt% TiO_2-NCM microspheres. (**h**,**i**) HRTEM images of 5 wt% TiO_2-NCM.

The constant current charge–discharge curves, cyclic stability, and rate performance of pristine NCM622, 2 wt%, 5 wt%, and 8 wt% TiO_2-NCM samples are shown in Figure 6a–d. In Figure 6a–d, all samples exhibit a plateau region in the first discharge curve, related to the redox reaction between Ni^{2+}/Ni^{4+} and Co^{3+}/Co^{4+} brought about by deintercalation and intercalation of Li^+ ions in the crystal lattice. The first cyclic discharge capacity of the 5 wt% TiO_2-NCM at 0.3 C is 183.5 mAh g^{-1}, which is higher than that of the pristine NCM622 of 179.2 mAh g^{-1}, and the average Coulombic efficiency (CE) of 5 wt% TiO_2-NCM can reach 100%. After 100 cycles, the pristine NCM622 shows a discharge capacity of 145 mAh g^{-1}, whereas 5 wt% TiO_2-NCM can maintain a discharge capacity of 163.9 mAh g^{-1}. The above

results indicate that the 5 wt% TiO_2-NCM has an excellent reversible specific capacity compared to the pristine NCM622. Furthermore, in Figure 6a–d, the voltage plateau of NCM811 also has a more substantial decline with the increase in the number of cycle turns. The charge–discharge curves of 2 wt% and 5 wt% TiO_2-NCM electrode materials are more compact, and the voltage and specific capacity decay more slowly. However, the voltage plateau of the 8 wt% TiO_2-NCM electrode material also has a large decline with the increase in the coating amount, which may be due to the drastic side reactions in the material with the increase in the TiO_2 coating amount [31]. This proves that the moderate amount of TiO_2 coating has a better protective effect on the material, isolating the direct contact between the active substance and the electrolyte, reducing the occurrence of side reactions, lowering the interfacial impedance, and reducing the polarisation of TiO_2-NCM electrode material [28].

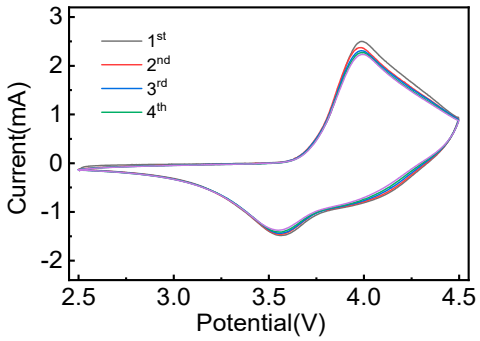

Figure 5. CV curves of 5 wt% TiO_2-NCM.

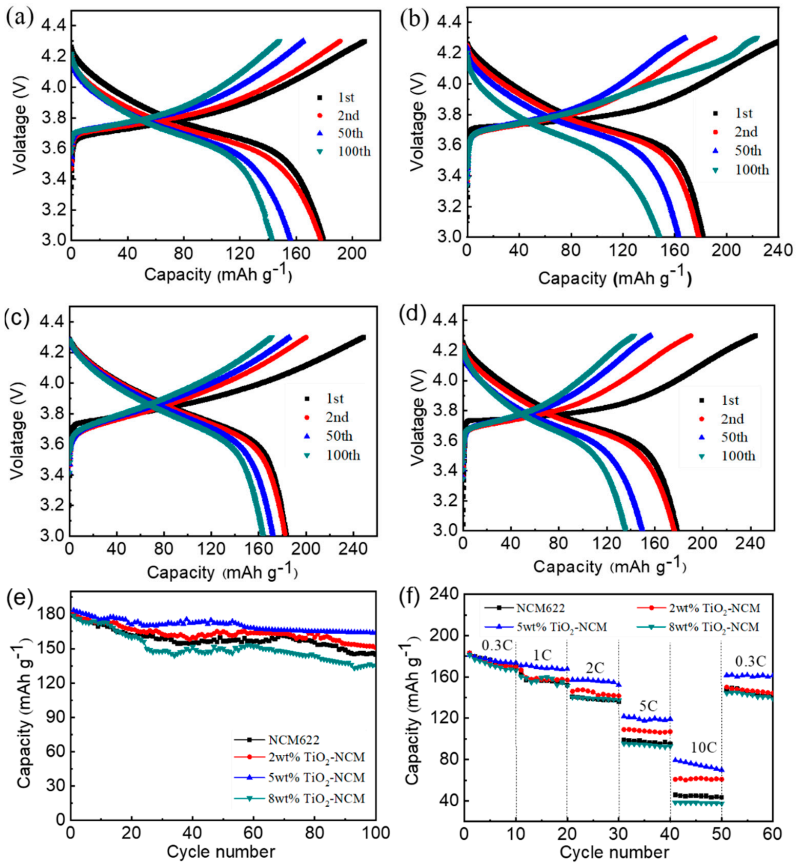

Figure 6. The charge-discharge curves of (**a**) NCM622, (**b**) 2 wt% TiO_2-NCM, (**c**) 5 wt% TiO_2-NCM, and (**d**) 8 wt% TiO_2-NCM samples. (**e**) The long-term cycle of NCM, 2 wt% TiO_2-NCM, 5 wt% TiO_2-NCM, and 8 wt% TiO_2-NCM samples at 0.3 C. (**f**) Rate performance of NCM, 2 wt% TiO_2-NCM, 5 wt% TiO_2-NCM, and 8 wt% TiO_2-NCM samples at different current densities.

Figure 6e shows the cycling stability of the pristine NCM622, 2 wt%, 5 wt%, and 8 wt% TiO_2-NCM samples after 100 cycles at 0.3 C. The cycling stability after 100 cycles at 0.3 C is shown in Table S1, where the 5 wt% TiO_2-NCM622 consistently maintains higher capacity and better cycling stability. For the NCM622 electrode, the reversible specific capacity decreases to 145 mAh g^{-1} after 100 cycles, whereas the 5 wt% TiO_2-NCM electrode still releases a reversible specific capacity of 163.9 mAh g^{-1} after 100 cycles, with a total capacity retention rate of 89.3%. The initial coulombic efficiency (ICE) of NCM622, 2 wt% TiO_2-NCM, 5 wt% TiO_2-NCM, and 8 wt% TiO_2-NCM samples are shown in Table S1, showing that the four kinds of materials exhibit ICE of 80.9, 83.0, 89.3, 75.7%, respectively. In general, the TiO_2-coated NCM electrodes exhibit higher ICEs compared with bare NCM, except that the 8 wt% TiO_2-NCM sample behaves with lower ICE, as shown in Table S1. This indicates that more TiO_2 coating content is not beneficial to the ICE improvement. Figure S4 shows the CE of the four kinds of materials within 100 cycles. In general, the CEs of TiO_2-coated NCM electrodes are close to 100% except for several cycles. The multiplicity performance of the samples is shown in Figure 6f. In general, the TiO_2-NCM electrodes exhibit better rate performance compared with bare NCM622. The 5 wt% TiO_2-NCM sample exhibits the best rate performance, with a discharge-specific capacity of an average of 70 mAh g^{-1} at a rate of 10.0 C, compared with ~35 mAh g^{-1} for bare NCM. The as-synthesized 5 wt% TiO_2-NCM exhibits the best electrochemical performance compared with other TiO_2-coated NCM electrodes, as shown in Table 2. The 8 wt% TiO_2-NCM sample exhibits the worst rate performance, indicating that the larger coating content of TiO_2 is diverse to the enhancement of electrochemical performance. The appropriate TiO_2 coating of NCM622 has the lowest cation mixing and highly ordered lamellar structure, which is conducive to the dislodgement and embedding of Li-ions, and the diffusion kinetics of Li-ion is faster; thus, the sample has the best rate performance [26].

Table 2. The discharge specific capacity and coulombic efficiency of NCM622 and TiO_2-coated NCM samples at 0.3 C.

Sample	Discharge Specific Capacity (mAh g^{-1})		Columbic Efficiency (%)
	1st	100th	
NCM622	179.2	145	80.9
2 wt% TiO_2-NCM	181.9	151	83.0
5 wt% TiO_2-NCM	183.5	163.9	89.3
8 wt% TiO_2-NCM	178.7	135.3	75.7

Figure 7 shows the cycling performance of NCM622 and 5 wt% TiO_2-NCM622 materials (at 3.0–4.6 V, 0.5 C). As can be seen from the figure, after 150 cycles, the 5 wt% TiO_2-NCM622 cathode material still releases a discharge-specific capacity of 107.3 mAh g^{-1}, which is higher than the unmodified NCM622 material (80.8 mAh g^{-1}). At the beginning of the cycle, the two materials have similar cycle tendencies. As the number of cycles is increased, the capacity of unmodified NCM622 decays more seriously, and the voltage plateau gradually disappears during the cycling process, resulting in a more serious polarisation phenomenon. In contrast, 5 wt% TiO_2-NCM622 electrode material shows a smaller degree of electrochemical performance degradation. This is mainly attributed to the fact that the appropriate amount of TiO_2 coating layer avoids the contact between the active material and the electrolyte, inhibits the dissolution of transition metals and the side reaction with the electrolyte, stabilizes the material structure, reduces the dynamic mixing of cations, and improves the cycling and multiplicity performance of the material [34].

A comparison of performance with various NCM cathodes reported previously by other researchers is summarized in Table S2, highlighting the better electrochemical performance of TiO_2-coated NCM electrodes in this study.

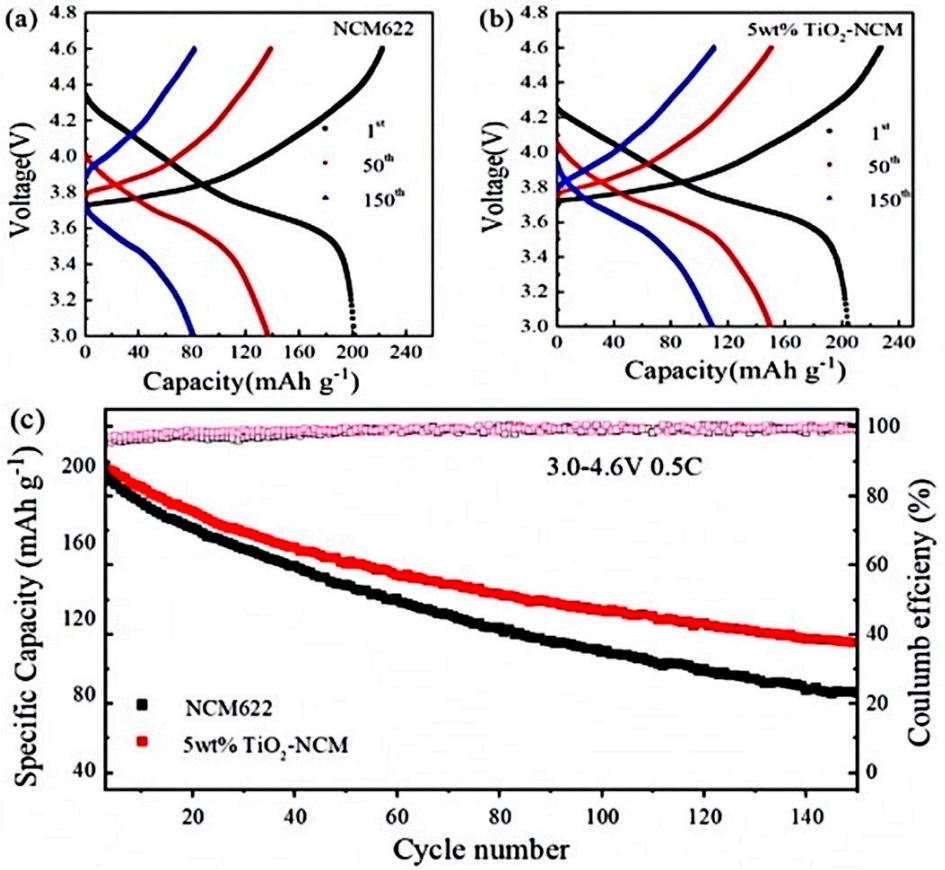

Figure 7. The charge-discharge curves of (**a**) NCM622, (**b**) 5 wt% TiO_2-NCM sample, and (**c**) cyclic curve under 0.5 C and 4.6 V conditions.

Electrochemical impedance spectroscopy (EIS) was performed to analyze the kinetics of NCM622 and TiO_2-modified NCM materials. As shown in Figure 8a, the Nyquist plots of pristine NCM622, 2 wt%, 5 wt%, and 8 wt% TiO_2-NCM samples all contain two cross-sections, which are the high-frequency region and low-frequency region cross-sections, respectively [35]. The semicircle in the high-frequency region indicates the charge transfer resistance (R_{ct}); the diagonal line in the low-frequency region indicates the diffusion impedance of lithium ions inside the cathode material [36,37]. The specific R_{ct} values are shown in Table S2. It can be found that the 5 wt% TiO_2-NCM electrode has the smallest charge transfer resistance. The straight line in the low-frequency region corresponds to the Warburg resistance (A_w) of the diffusion of Li-ion inside the electrode, and the larger the slope is, the larger the Warburg resistance, as shown in Figure 8b. The Warburg coefficients of the four electrodes, NCM622, 2 wt% TiO_2-NCM, 5 wt% TiO_2-NCM, and 8 wt% TiO_2-NCM, are 191, 142, 113, and 258 $\Omega\ s^{-1/2}$, respectively, by fitting, which proves that the 5 wt% TiO_2-NCM has a faster electrochemical kinetics. The appropriate amount of TiO_2 coating layer avoids the contact between the active material and the electrolyte, inhibits the dissolution of transition metals and the side reaction with the electrolyte, stabilizes the material structure, reduces the dynamic mixing of cations, and improves the electrochemical performance of the material [38,39].

The fade mechanism of electrochemical properties for bare NCM and improvement mechanism for TiO_2-coated NCM materials need to be conducted through several characterization techniques, especially at a higher cutoff voltage of 4.6 V. Further work will also include the combination of some modification strategies for improving the electrochemical performance of NCM materials.

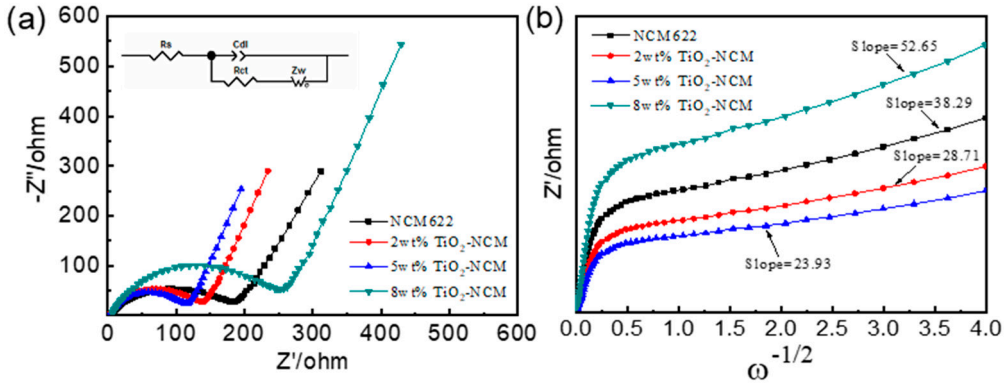

Figure 8. (**a**) Nyquist plots of NCM, 2 wt% TiO_2-NCM, 5 wt% TiO_2-NCM, and 8 wt% TiO_2-NCM electrodes (the inset is an equivalent circuit.); (**b**) the linear fitting diagram of the Warburg impedance.

4. Conclusions

In summary, TiO_2-coated NCM material cathode materials were prepared by a simple hydrolysis reaction. The effects of different amounts of TiO_2 coating on the morphology, structure, and electrochemical properties of the products were studied.Compared with the unmodified sample, the cycling stability of the modified TiO_2-modified $LiNi_{0.6}Co_{0.2}Mn_{0.2}O_2$ samples is significantly improved. When the amount of TiO_2 coating reaches 5.0%, the 5wt% TiO_2-NCM material has a discharge capacity of 163.9 mAh g^{-1} after 150 cycles and shows better electrochemical properties with a high cutoff voltage (3.0–4.6 V). The improvement of the cycling performance of TiO_2-coated NCM is mainly attributed to the following reasons: (1) TiO_2 has a stable structure, which effectively improves the overall mechanical stability of the material through the close bonding with NCM622; (2) the TiO_2 coating layer stabilizes the interface between the electrode and the electrolyte and isolates the active substance from the electrolyte. In addition, a small amount of Ti^{4+} is doped into the crystal lattice of NCM622 during the high-temperature roasting process, which maintains the integrity of the crystal structure of NCM622 and plays the role of supporting the structure.

Supplementary Materials: The following supporting information can be downloaded at: https://www.mdpi.com/article/10.3390/ma17246222/s1. Experimental parts: characterizations and electrochemical measurements. Figure S1. Local magnification XRD patterns of peaks (a) (003) and (b) (104). Figure S2. The XPS spectra of bare NCM622: (a) survey spectrum; (b) Ni 2*p*; (c) Co 2*p*; (d) Mn 2*p*. Figure S3. CV curves of NCM622. Figure S4. Coulombic efficiency of NCM622, 2 wt% TiO_2-NCM, 5 wt% TiO_2-NCM, and 8 wt% TiO_2-NCM samples. Table S1. The discharge specific capacity and initial coulombic efficiency of NCM622 and TiO_2-coated NCM samples at 0.3 C. Table S2. Comparison of electrochemical performances of part of coated $LiNi_{0.6}Co_{0.2}Mn_{0.2}O_2$ (NCM) with previous work reported for LIB. Table S3. The Charge transfer resistance (R_{ct})of NCM and TiO_2-coated NCM samples. References [40–42] are cited in the Supplementary Materials.

Author Contributions: Conceptualization, L.L. and Z.L.; methodology, L.L., Z.L. and H.Z.; investigation, Z.L., Z.K., M.Y. and J.L.; resources, L.L.; writing—original draft preparation, L.L.; writing—review and editing, L.L., S.W. and H.L.; supervision, L.L.; project administration, S.W. and H.L.; funding acquisition, L.L. All authors have read and agreed to the published version of the manuscript.

Funding: This work was financially supported by the Key Laboratory for Research and Development of new lithium-ion battery materials (2023-028), Project of the Three Gorges Laboratory of Hubei Province (SK240004), the Joint Foundation Project of Bijie City Science and Technology Burean and Guizhou University of Engineering Science (BiKeLianhe[2023]39), and Joint Fund of Bijie City and Guizhou University of Engineering Science (BiKeLianhe[2023]12th).

Institutional Review Board Statement: Not applicable.

Informed Consent Statement: Not applicable.

Data Availability Statement: The original contributions presented in this study are included in the article/Supplementary Materials. Further inquiries can be directed to the corresponding authors.

Acknowledgments: We are very grateful to all the people who gave us valuable advice while we were writing this paper.

Conflicts of Interest: The authors declare no conflicts of interest.

References

1. Shi, C.M.; Takeuchi, S.; Alexander, G.V.; Hamann, T.; O'Neill, J.; Dura, J.A.; Wachsman, E.D. High Sulfur Loading and Capacity Retention in Bilayer Garnet Sulfurized-Polyacrylonitrile/Lithium-Metal Batteries with Gel Polymer Electrolytes. *Adv. Energy Mater.* **2023**, *13*, 2301656. [CrossRef]
2. Lu, J.Y.; Xu, C.; Dose, W.; Dey, S.; Wang, X.H.; Wu, Y.H.; Li, D.P.; Ci, L.J. Microstructures of layered Ni-rich cathodes for lthium-ion batteries. *Chem. Soc. Rev.* **2024**, *53*, 4707–4740. [CrossRef] [PubMed]
3. You, B.; Wang, Z.; Shen, F.; Chang, Y.; Peng, W.; Li, X.; Guo, H.; Hu, Q.; Deng, C.; Yang, S.; et al. Research progress of sigle-crystal nickel-rich cathode materials for lithium-ion batteries. *Small Methods* **2021**, *5*, 2100234. [CrossRef] [PubMed]
4. Song, Y.Z.; Wang, L.; Sheng, L.; Ren, D.S.; Liang, H.M.; Li, Y.D.; Wang, A.P.; Zhang, H.; Xu, H.; He, X.M. The significance of mitigating crosstalk in lithium-ion batteries: A review. *Energy Environ. Sci.* **2023**, *16*, 1943–1963. [CrossRef]
5. Mei, P.; Zhang, Y.; Zhang, W. Low-temperature lithium-ion batteries: Challenges and progressof surface/interface modifications for advanced performance. *Nanoscale* **2023**, *15*, 987–997. [CrossRef] [PubMed]
6. Li, J.; Zhong, W.; Deng, Q.; Zhang, Q.; Yang, C. Recent progress in synthesis and surface modification of nickel-rich layered oxide cathode materials for lithium-ion batteries. *Int. J. Extrem. Manuf.* **2022**, *4*, 042004. [CrossRef]
7. Moryson, Y.; Walther, F.; Sann, J.; Mogwitz, B.; Ahmed, S.; Burkhardt, S.; Chen, L.; Klar, P.J.; Volz, K.; Fearn, S.; et al. Analyzing Nanometer-Thin Cathode Particle Coatings for Lithium-Ion Batteries—The Example of TiO_2 on NCM622. *ACS Appl. Energy Mater.* **2021**, *4*, 7168–7181. [CrossRef]
8. Wang, W.C.; Lee, C.H.; Yu, D.N.; Kondo, Y.; Miyahara, Y.; Abe, T.; Miyazaki, K. Effects of a Solid Solution Outer Layer of TiO_2 on the Surface and Electrochemical Properties of $LiNi_{0.6}Co_{0.2}Mn_{0.2}O_2$ Cathodes for Lithium-Ion Batteries through the Use ofThin-Film Electrodes. *ACS Appl. Energy Mater.* **2022**, *5*, 5117–5126. [CrossRef]
9. Men, L.J.; Feng, S.Y.; Zhang, J.F.; Luo, X.B.; Zhou, Y.F. Asyste maticreview of efficientre cycling for the cathode materials of spent lithium-ion batteries: Process inten sification technologies beyond traditional methods. *Green Chem.* **2024**, *26*, 1170–1193. [CrossRef]
10. Jang, S.-H.; Lee, K.-J.; Mun, J.; Han, Y.-K.; Yim, T. Chemically-induced cathode-electrolyte inter phase created by lithium salt coating on Nickel-rich layered oxides cathode. *J. Power Sources* **2019**, *410*, 15–24. [CrossRef]
11. Marriam, I.; Tebyetekerwa, M.; Chathuranga, H.; Sun, K.G.; Du, A.J.; Yan, C. Nickel-Rich Cathode Yarn for Wearable Lithium-Ion Batteries. *Adv. Fiber Mater.* **2024**, *6*, 341–353. [CrossRef]
12. Gu, H.; Mu, Y.; Zhang, S.T.; Li, Y.Q.; Hu, H.L.; Zhu, X.Y.; Meng, W.J.; Qiu, J.Y.; Ming, H. Enhanced thermal safety and rate capability of nickel-rich cathodes via optimal Nb-doping strategy. *Electrochim. Acta* **2024**, *487*, 144216. [CrossRef]
13. Li, X.; Ge, W.J.; Zhang, K.K.; Peng, G.C.; Fu, Y.X.; Ma, X.G. Comprehensive study of tantalum doping on morphology, structure, and electrochemical performance of Ni-rich cathode materials. *Electrochim. Acta* **2022**, *403*, 139653. [CrossRef]
14. Zhang, X.; Belharouak, I.; Li, L.; Yu, L.; Elam, J.W.; Nie, A.; Chen, X.; Yassar, R.S.; Axelbaum, R.L. Structural and electrochemical study of Al_2O_3 and TiO_2 coated $Li_{1.2}Ni_{0.13}Mn_{0.54}Co_{0.13}O_2$ cathode material using ALD. *Adv. Energ. Mater.* **2013**, *3*, 1299–1307. [CrossRef]
15. Ge, W.J.; Fu, Y.X.; Ma, X.G.; Li, X.; Peng, G.C. Dualmodification of $LiNi_{0.6}Co_{0.2}Mn_{0.2}O_2$ with $MgHPO_4$ as a high-performance cathode material for Li-ion batteries. *Energy Adv.* **2022**, *1*, 28–37. [CrossRef]
16. Cao, J.; Li, Y.; Wang, L.J.; Li, J.; Qiao, Y.M.; Zhu, L.P.; Zhang, S.N.; Yan, X.X.; Xie, H.Q. Enhanced electrochemical performances of $Li_{1.2}Ni_{0.13}Co_{0.13}Mn_{0.54}O_2$ cathode material coated with ZrO_2. *Ionics* **2023**, *51*, 51–60. [CrossRef]
17. Yao, L.; Liang, F.; Jin, J.; Chowdari, B.V.R.; Yang, J.H.; Wen, Z.Y. Improved electrochemical property of Ni-rich $LiNi_{0.6}Co_{0.2}Mn_{0.2}O_2$ cathode via in-situ ZrO_2 coating for high energy density lithium-ion batteries. *Chem. Eng. J.* **2020**, *389*, 124403. [CrossRef]
18. Wang, L.; Liang, J.; Zhang, X.; Li, S.; Wang, T.; Ma, F.; Han, J.; Huang, Y.; Li, Q. An effectivedual-modification strategytoenhance the performance of $LiNi_{0.6}Co_{0.2}Mn_{0.2}O_2$ cathode for Li-ion batteries. *Nanoscale* **2021**, *13*, 4670–4677. [CrossRef]
19. Yu, H.; He, X.Q.; Liang, X.H. AlF_3-Al_2O_3 ALDThin-Film-Coated $Li_{1.2}Mn_{0.54}Co_{0.13}Ni_{0.13}O_2$ Particles for Lithium-Ion Batteries: Long-Term Protection. *ACS Appl. Mater. Interfaces* **2022**, *14*, 3991–4003. [CrossRef] [PubMed]
20. Yang, H.; Zhang, H.; Zhao, W. Improvement of electrochemical performance of $LiNi_{0.5}Co_{0.2}Mn_{0.3}O_2$ byLaF_3 coating at highcut-offvoltage. *Ionics* **2023**, *29*, 1335–1345. [CrossRef]
21. Tang, W.; Peng, Z.; Shi, Y.; Sheng, X.; Shuai, H.T.; Zhou, S.; Kong, Y.; Yan, K.P.; Lu, T.C.; Wang, G.X. Enhanced cyclability andsafety performance of $LiNi_{0.6}Co_{0.2}Mn_{0.2}O_2$ at elevated temperature by $AlPO_4$ modification. *J. Alloys Compd.* **2019**, *810*, 151834. [CrossRef]
22. Zhang, W.; Liang, L.; Zhao, F.; Liu, Y.; Hou, L.R.; Yuan, C.Z. Ni-rich $LiNi_{0.8}Co_{0.1}Mn_{0.1}O_2$ coated withLi-ion conductive Li_3PO_4 as competitive cathodes for high-energy-density lithium-ion batteries. *Electrochim. Acta* **2020**, *340*, 135871. [CrossRef]

23. Cho, W.; Kim, S.M.; Lee, K.W.; Song, J.H.; Jo, Y.N.; Yim, T.; Kim, H.; Kim, J.-S.; Kim, Y.-J. Investigation of new manganese orthophosphate $Mn_3(PO_4)_2$ coating for nickel-rich $LiNi_{0.6}Co_{0.2}Mn_{0.2}O_2$ cathode and improvement of its thermal properties. *Electrochim. Acta* **2016**, *198*, 77–83. [CrossRef]
24. Yang, X.; Meng, Q.; Zhang, Y.j.; Dong, P.; Fei, Z.T.; Li, C.C.; Wang, J.J.; Li, W.B.; Li, X.F.; Xu, K.H.; et al. Samariumoxide coating with enhanced lithium storage of regenerated $LiNi_{0.6}Co_{0.2}Mn_{0.2}O_2$. *Surf. Interfaces* **2023**, *42*, 103405. [CrossRef]
25. Venkatachalam, P.; Duru, K.K.; Rangarajan, M.; Sangaraju, S.; Maram, P.S.; Kalluri, S. $LiNbO_3$ coating on Mg-doped NCM-622 cathode—Adual modification to enhance the electrochemical performance at higher voltage for lithium-ion batteries. *J. Solid State Electrochem.* **2024**, *28*, 3509–3515. [CrossRef]
26. Huang, K.; Zhou, J.X.; Yang, H.L.; Xie, T.Z.; Lan, T.; Ong, S.C.; Jiang, H.; Zeng, Y.B.; Guo, H.; Zhang, Y. TiO_2–LiF compositecoating for improving NCM622 cathode cycling stability: One-step construction. *RSC Adv.* **2023**, *13*, 33905–33910. [CrossRef]
27. Li, W.W.; Zhang, X.J.; Si, J.J.; Yang, J.; Sun, X.Y. TiO_2-coated $LiNi_{0.9}Co_{0.08}Al_{0.02}O_2$ cathode materials with enhanced cycle performance for Li-ion batteries. *Rare Met.* **2021**, *40*, 1719–1726. [CrossRef]
28. Wang, W.Z.; Wu, L.Y.; Li, Z.W.; Huang, K.S.; Jiang, J.M.; Chen, Z.Y.; Qi, X.D.; Dou, H.; Zhang, X.G. In Situ Tuning Residual Lithium Compounds and Constructing TiO_2 Coating for Surface Modification of a Nickel-Rich Cathode toward High-Energy Lithium-Ion Batteries. *ACS Appl. Energy Mater.* **2020**, *12*, 12423–12432. [CrossRef]
29. Qin, C.C.; Cao, J.L.; Chen, J.; Dai, G.L.; Wu, T.F.; Chen, Y.B.; Tang, Y.F.; Li, A.D.; Chen, Y.F. Improvement of electrochemicalperformance of nickel rich $LiNi_{0.6}Co_{0.2}Mn_{0.2}O_2$ cathode active material by ultrathin TiO_2 coating. *Dalton Trans.* **2016**, *45*, 9669–9675. [CrossRef] [PubMed]
30. You, L.Z.; Wen, Y.; Li, G.X.; Chu, B.B.; Wu, J.H.; Huang, T.; Yu, A.S. Nano-TiO_2 coated single-crystal $LiNi_{0.65}Co_{0.15}Mn_{0.2}O_2$ for lithium-ion batteries with a stable structure and excellent cycling performance at a high cut-off voltage. *J. Mater. Chem. A* **2022**, *10*, 5631–5641. [CrossRef]
31. Mo, Y.; Guo, L.J.; Jin, H.F.; Du, B.D.; Cao, B.K.; Chen, Y.G.; Li, D.; Chen, Y. Improved cycling stability of $LiNi_{0.6}Co_{0.2}Mn_{0.2}O_2$ through microstructure consolidation by TiO_2 coating for Li-ion batteries. *J. Power Sources* **2020**, *448*, 227439. [CrossRef]
32. Chang, L.J.; Hou, Z.L.; Yang, W.; Yang, R.F.; Wei, A.L.; Luo, S.H. The theory guides the doping of rare earth elements in the bulk phase of LiNi0.6Co0.2Mn0.2O2 to reach the theoretical limit of energy density. *J. Colloid Interface Sci.* **2025**, *682*, 340–352. [CrossRef] [PubMed]
33. Yang, W.T.; Li, R.F.; Chen, Y.; Song, L.J.; Lu, X.Y.; Jiang, Q. Preparation of a high performance $LiNi_{0.6}Co_{0.2}Mn_{0.2}O_2$ cathode material by using citric acid as a complexing agent. *Green Chem.* **2023**, *25*, 1085–1095.
34. Jia, S.X.; Xue, J.X.; Huo, H.; Zhou, J.J.; Li, L. Tailoring the interface of lithium metal batteries with an in situ formed gel polymer electrolyte. *J. Mater. Chem. A* **2024**, *12*, 15430–15439. [CrossRef]
35. Kim, S.; Lee, K.; Kim, K.; Lee, S.S.S.; Fortner, D.; An, H.; Son, Y.; Hwang, H.; Han, Y.; Myung, Y.; et al. Reductive Dissolution of NCM Cathode through Anaerobic Respiration by Shewanella putrefaciens. *Environ. Sci. Technol.* **2024**, *58*, 18345–18355. [CrossRef] [PubMed]
36. Truong, B.; Wu, Y.; Hung, T. The effect of lithium-excess on Ni-rich $LiNi_{0.6}Co_{0.2}Mn_{0.2}O_2$ cathode materials prepared by a Taylor flow reactor. *Electrochim. Acta* **2021**, *391*, 138982–138994. [CrossRef]
37. Su, M.Y.; Dong, X.W.; Dai, X.Y.; Huang, B.B.; Shen, M.; Xu, T.; Liu, Q.B. Enhanced Cycling Performance of Spinel $LiNi_{0.5}Mn_{1.5}O_4$ Cathodes through Mg-Mn Hetero-Valent Doping via Microwave Sol-Gel Method. *Materials* **2024**, *17*, 4714. [CrossRef] [PubMed]
38. Feng, Z.; Zhang, S.; Rajagopalan, R.; Huang, X.B.; Ren, Y.R.; Sun, D.; Wang, H.Y.; Tang, Y.G. Dual-Element-Modified Single-Crystal $LiNi_{0.6}Co_{0.2}Mn_{0.2}O_2$ as a Highly Stable Cathode for Lithium-Ion Batteries. *ACS Appl. Mater. Interfaces* **2021**, *13*, 43039–43050. [CrossRef]
39. Jo, M.; Oh, P.; Kim, J.; Choi, J.H.; Kim, S.; Ha, S.; Son, Y. Electrochemical lithium storage performance at high voltage and temperature of $LiNi_{0.6}Co_{0.2}Mn_{0.2}O_2$ cathode for Lithium-ion batteries by facile $Mn_3(PO_4)_2$ dry coating. *Appl. Surf. Sci.* **2023**, *613*, 156018. [CrossRef]
40. Huang, G.J.; Zhong, Y.; Xia, X.H.; Wang, X.L.; Gu, C.D.; Tu, J.P. Surface-modified and sulfide electrolyte-infiltrated $LiNi_{0.6}Co_{0.2}Mn_{0.2}O_2$ cathode for all-solid-state lithium batteries. *J. Colloid Interface Sci.* **2023**, *632*, 11–18. [CrossRef]
41. Diao, H.H.; Jia, M.Y.; Zhao, N.; Guo, X.X. $LiNi_{0.6}Co_{0.2}Mn_{0.2}O_2$ Cathodes Coated with Dual-Conductive Polymers for High-Rate and Long-Life Solid-State Lithium Batteries. *ACS Appl. Mater. Interfaces* **2022**, *14*, 24929–24937. [CrossRef]
42. Liu, W.M.; Zeng, S.S.; Wang, P.P.; Huang, J.; Shen, B.; Qin, M.L.; Wang, W.G.; Tang, Z.X. Dual-coated single-crystal $LiNi_{0.6}Co_{0.2}Mn_{0.2}O_2$ as high-performance cathode materials for lithium-ion batteries. *J. Solid State Electrochem.* **2024**. [CrossRef]